NASA/TM—20230009397

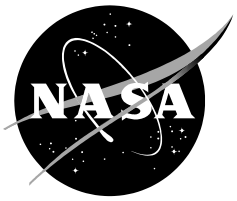

Commercial-Off-The-Shelf Small-Form Factor Organic LED and Liquid Crystal Displays Displacement Damage and Total Ionizing Dose Test Report

Landen D. Ryder

Edward J. Wyrwas

Geraldo A. Cisernos

July 2023

NASA STI Program Report Series

The NASA STI Program collects, organizes, provides for archiving, and disseminates NASA's STI. The NASA STI program provides access to the NTRS Registered and its public interface, the NASA Technical Reports Server, thus providing one of the largest collections of aeronautical and space science STI in the world. Results are published in both non-NASA channels and by NASA in the NASA STI Report Series, which includes the following report types:

- TECHNICAL PUBLICATION. Reports of completed research or a major significant phase of research that present the results of NASA Programs and include extensive data or theoretical analysis. Includes compilations of significant scientific and technical data and information deemed to be of continuing reference value. NASA counterpart of peer-reviewed formal professional papers but has less stringent limitations on manuscript length and extent of graphic presentations.

- TECHNICAL MEMORANDUM. Scientific and technical findings that are preliminary or of specialized interest, e.g., quick release reports, working papers, and bibliographies that contain minimal annotation. Does not contain extensive analysis.

- CONTRACTOR REPORT. Scientific and technical findings by NASA-sponsored contractors and grantees.

- CONFERENCE PUBLICATION. Collected papers from scientific and technical conferences, symposia, seminars, or other meetings sponsored or co-sponsored by NASA.

- SPECIAL PUBLICATION. Scientific, technical, or historical information from NASA programs, projects, and missions, often concerned with subjects having substantial public interest.

- TECHNICAL TRANSLATION. English-language translations of foreign scientific and technical material pertinent to NASA's mission.

Specialized services also include organizing and publishing research results, distributing specialized research announcements and feeds, providing information desk and personal search support, and enabling data exchange services.

For more information about the NASA STI program, see the following:

- Access the NASA STI program home page at http://www.sti.nasa.gov

- Help desk contact information:

https://www.sti.nasa.gov/sti-contact-form/ and select the "General" help request type.

NASA/TM—20230009397

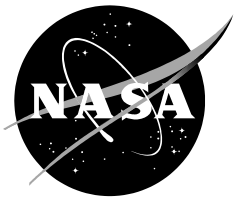

Commercial-Off-The-Shelf Small-Form Factor Organic LED and Liquid Crystal Displays Displacement Damage and Total Ionizing Dose Test Report

Landen D. Ryder
Goddard Space Flight Center, Greenbelt, MD

Edward J. Wyrwas
Science Systems and Applications, Inc., Lanham MD

Geraldo A. Cisernos
Johnson Space Center, Houston, TX

Test Date: 9/28/2022
Report Date: 6/27/2023

National Aeronautics and
Space Administration

Goddard Space Flight Center
Greenbelt, MD 20771

July 2023

Acknowledgments (optional)

This work was sponsored by the NASA GSFC Radiation Effects and Analysis Group and supported by the Displays Sustain Lunar Spacecraft Program.

Level of Review: This material has been technically reviewed by technical management.

Available from

NASA STI Program
Mail Stop 148
NASA's Langley Research Center
Hampton, VA 23681-2199

National Technical Information Service
5285 Port Royal Road
Springfield, VA 22161
703-605-6000

This report is available in electronic form at

https://radhome.gsfc.nasa.gov/

TABLE OF CONTENTS

1. INTRODUCTION

The push towards returning humans to the lunar surface and beyond necessitates further examination of technologies and challenges unique to human inhabitants. Electronic displays are one such technology that is critically positioned as an informational interchange between the electronic and human domains in a variety of applications. As manned missions look toward long-term infrastructure outside the safety of the magnetosphere, the impact of radiation-induced degradation for electronic displays must be considered to best serve the reliability requirements for use while also allowing for the size, weight, and power benefits of display technology advancements.

The purpose of this test campaign was to characterize commercial-off-the-shelf (COTS) electronic display technologies for radiation-induced degradation in the light emission component of the display (i.e. screen) via displacement damage dose (DDD) and total ionizing dose (TID). Four display technologies were irradiated during this test campaign: LCD with edge coupled light emitting diode (LED) backlight, passive matrix organic light emitting diode (OLED), mono-color LED dot matrices (blue and white), and reflective electronic ink or electronic paper displays (black/white and tri-color). Since the objective was to characterize radiation-induced degradation in the screen and not support electronics, the COTS display boards were modified such that support electronics were not within the path of the apertured proton beam (Fig. 1).

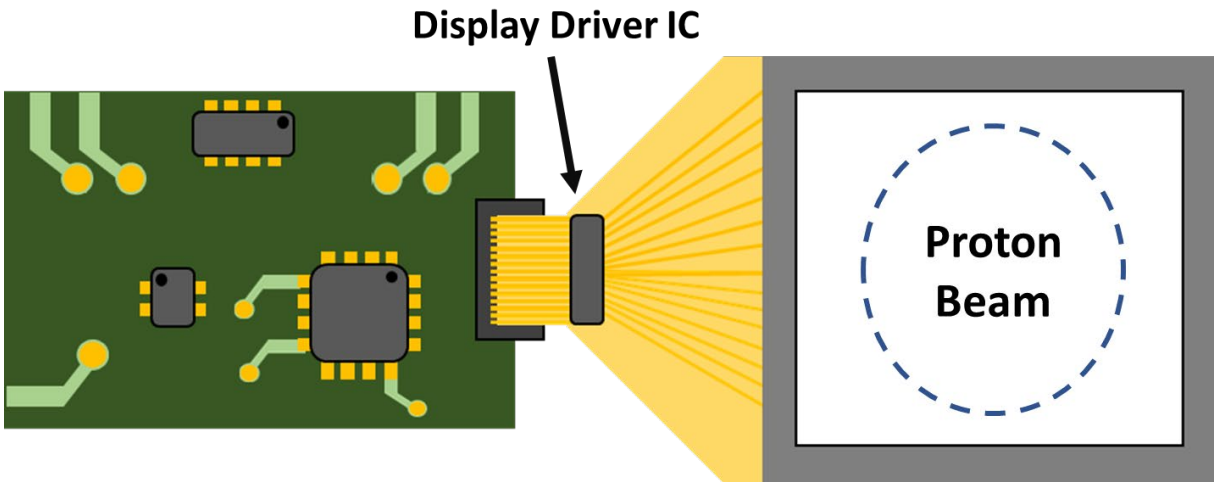

Figure 1: Notional schematic of display boards and the modifications used in this measurement campaign. The screen containing the individual pixels are attached to an electronic board and display driver IC with a flexible tape connector. This allows for “unfolding” the display to center the beam on the screen and avoid support electronics.

2. DEVICES TESTED

2.1. Part Background

For this test campaign, small COTS display hobbyist boards were selected to examine cumulative dose effects in OLED and TFT-LCD pixel technologies. These display boards are compatible with common microcontrollers and have publicly available libraries to facilitate development of test software for display driving. Additionally, the display screens are connected to the display control electronic boards via tape connectors which allows for physical manipulation of the prototype board for testing to control the region of the display that is being irradiated.

The OLED display used in this test campaign was the 1.5" (128x128 RGB pixel) 16-bit color OLED display board from Adafruit [1] (product ID: 1431) (Fig. 2). This board makes use of a SSD1351 driver chip to drive the display and interfaces with an off-board microcontroller via 4-wire write-only serial peripheral interface (SPI) connection. The display requires a 5V input power and logic levels and uses an on-board boost converter to provide the 12V required by the OLEDs. The light emission layer of the display screen is between two 800-micron glass layers that provide passivation, protection, and structural support.

The TFT-LCD display used in this test campaign was the 2.4" (240x320 RGB pixel) and 3.5" (320x480 RGB pixel) 16-bit color TFT-LCD display boards from Adafruit [2]-[3] (product IDs: 2478 and 2050 respectively) (Fig. 3). The LCD boards make use of a ILI9341 (2.4" display) and HXD8357 (3.5" display) driver chips to drive the displays and interface with an off-board microcontroller via SPI or 8-wire serial control connection. The display requires a 5V input power and logic levels and uses an on-board boost converter to provide the 25V required by the LED backlights and LCD control circuitry. This display relies on edge coupled LEDs to provide the backlight, the LEDs are not physically located behind the TFT layer in the screen. The TFT layer of the display screen is behind approximately 2.6 mm glass layer that provides passivation, protection, and structural support.

The electronic paper displays used in this test campaign were the monochrome and tricolor 1.54" (200x200 pixel) active matrix electronic paper display board from Adafruit [4]-[5] (product ID: 4196 and 4868) (Fig. 4). This board makes use of a SSD13681 driver chip to drive the display and interfaces with an off-board microcontroller via 4-wire write-only SPI connection. The display requires a 5V input power and logic levels and uses an on-board boost converter to provide the necessary voltage to the individual pixels. The reflective polymer of the display screen is between two 800-micron glass layers that provide passivation, protection, and structural support. There is no built in light emissive component for these display boards.

The mono-color LED dot matrices used in this test campaign was the 0.8" 8x8 white dot matrix and 1.2" 8x8 blue dot matrix based on InGaN LEDs sourced from Adafruit [6]-[7] (product IDs: 2478 and 2050 respectively) (Fig. 5). These dot matrix displays utilize a conduct network to electrical contact each LED, meaning there is no additional active electronics contained with the display. It should be noted there is a small plastic layer over each LED.

In addition to the differences in light emission layers, the displays used in this test campaign utilizes different pixel driving techniques. Conceptually, passive matrix displays utilize a grid of horizontal (rows) and vertical (columns) to provide electrical connection to pixels by sweeping through enabling individual row lines and using the column lines as a data bus to selectively forward bias OLEDs for the enabled row. In contrast, active matrix displays utilize transistors and capacitors at each pixel to individually address pixels and charge a storage capacitor that maintains the state of pixel while the pixel is not currently selected. A simplified pixel description for the displays examined in this test campaign is provided in Fig. 6. This distinction of driving mechanisms is notable as the presence of pixel transistors introduces the potential for total ionizing dose degradation of the transistor that could result in threshold voltage shifts.

Table 1: Part Identification Information

Qty	Part Number	Supplier	REAG ID	Description
4	Product ID: 1431	Adafruit	22-045	OLED Display Board
4	Product ID: 2478	Adafruit	22-046	TFT-LCD Display Board
1	Product ID: 2050	Adafruit	22-047	TFT-LCD Display Board
1	KWM-30881CBB	Lucky Light	22-049	Blue LED Matrix
3	KWM-20882XWB	Lucky Light	22-048	White LED Matrix
2	Product ID: 4196	Adafruit	22-050	Monochrome Electronic Paper
2	Product ID: 4868	Adafruit	22-051	Tricolor Electronic Paper

Figure 2: OLED boards used in this measurement campaign.

Figure 3: TFT-LCD boards used in this measurement campaign.

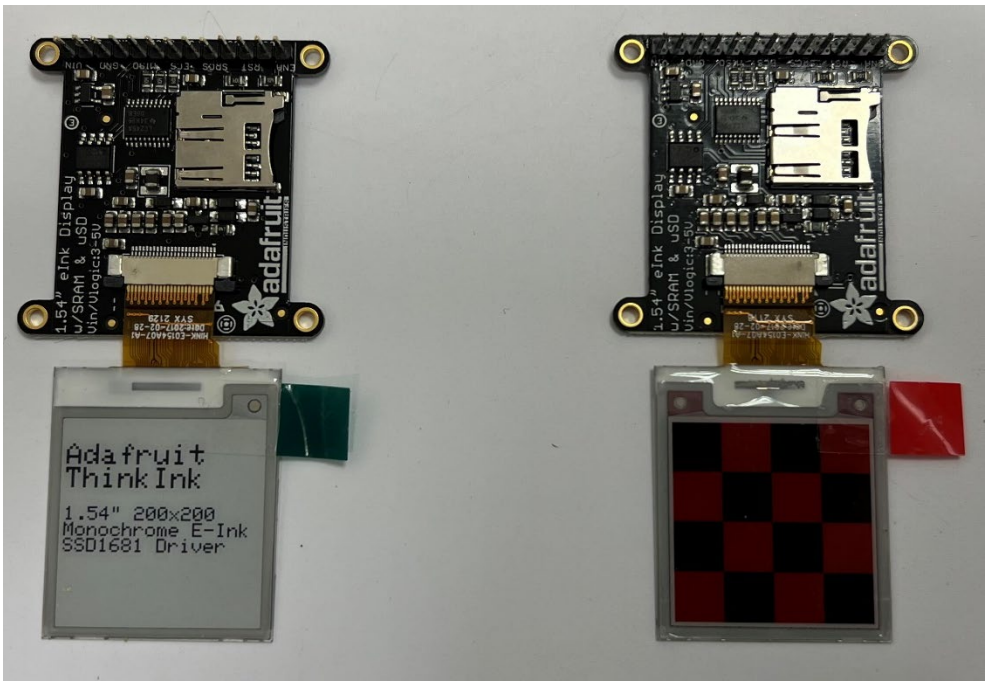

Figure 4: Monochrome and Tricolor eInk boards used in this measurement campaign.

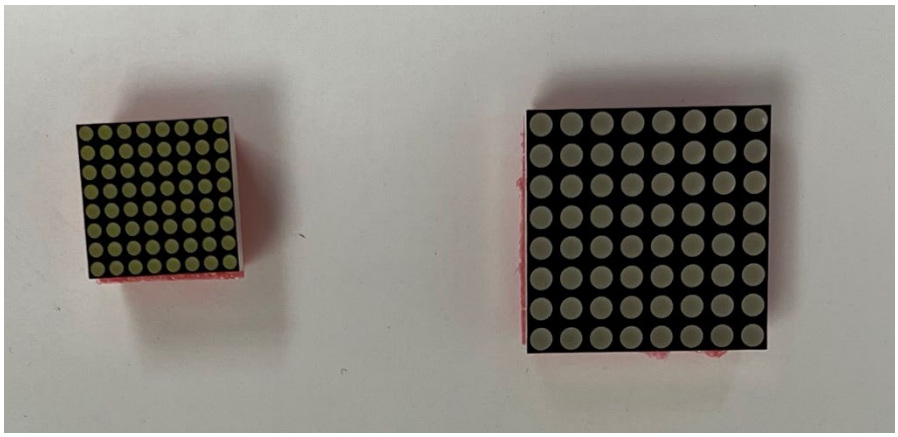

Figure 5: White (Left) and Blue (right) LED matrices used in this measurement campaign.

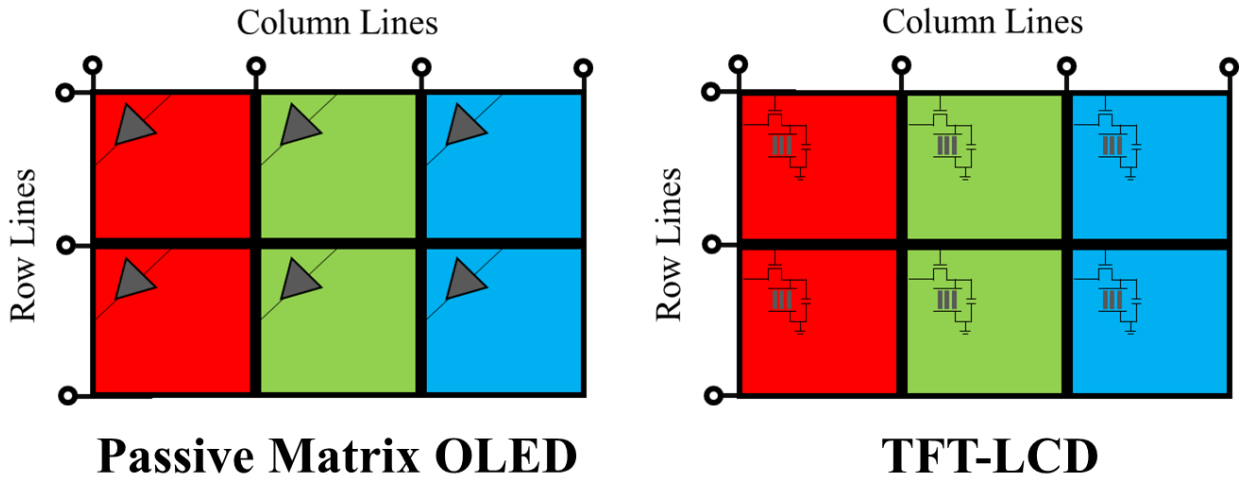

Figure 6: Notional schematic of passive matrix and active matrix display driving techniques. Note that active matrix TFT-LCDs introduce transistors at the pixel level not present in passive matrix displays.

2.2. Device Under Test (DUT) Information

Each display board selected for DDD and TID testing was irradiated with an apertured 64 MeV proton beam. Prior to any modification, a display board consisted of a screen connected to a tape connector that provided the necessary connections to driver ICs and any additional support electronics on a distinct printed circuit board (PCB); the display screen was affixed to the PCB via a small metallic facet, (TFT-LCD), small amount of tape (OLED), or a bonding epoxy (electronic paper). Care was taken to detach the screen from the board without damaging the tape connector and effectively configure the display screen and electronics board in the same plane. Display screens and support electronics were attached to a piece of protoboard with anti-static tape to allow for mounting in the beam line (depicted in Fig. 7-8). Onboard header pins allow for wire connections for power supply and microcontroller signals located away from the proton beam.

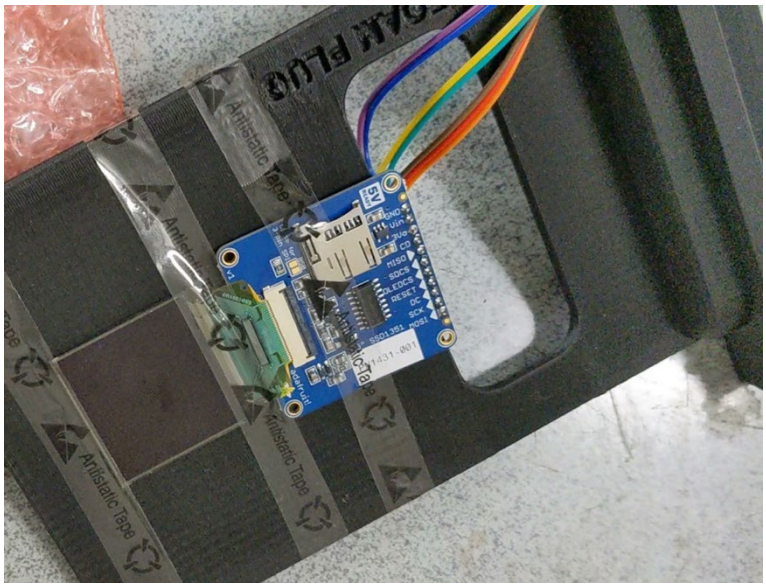

Figure 7: An example of mounting a display to a test tray for irradiation and characterization. Anti-static tap was utilized to securely mount the display board and screen to the tray.

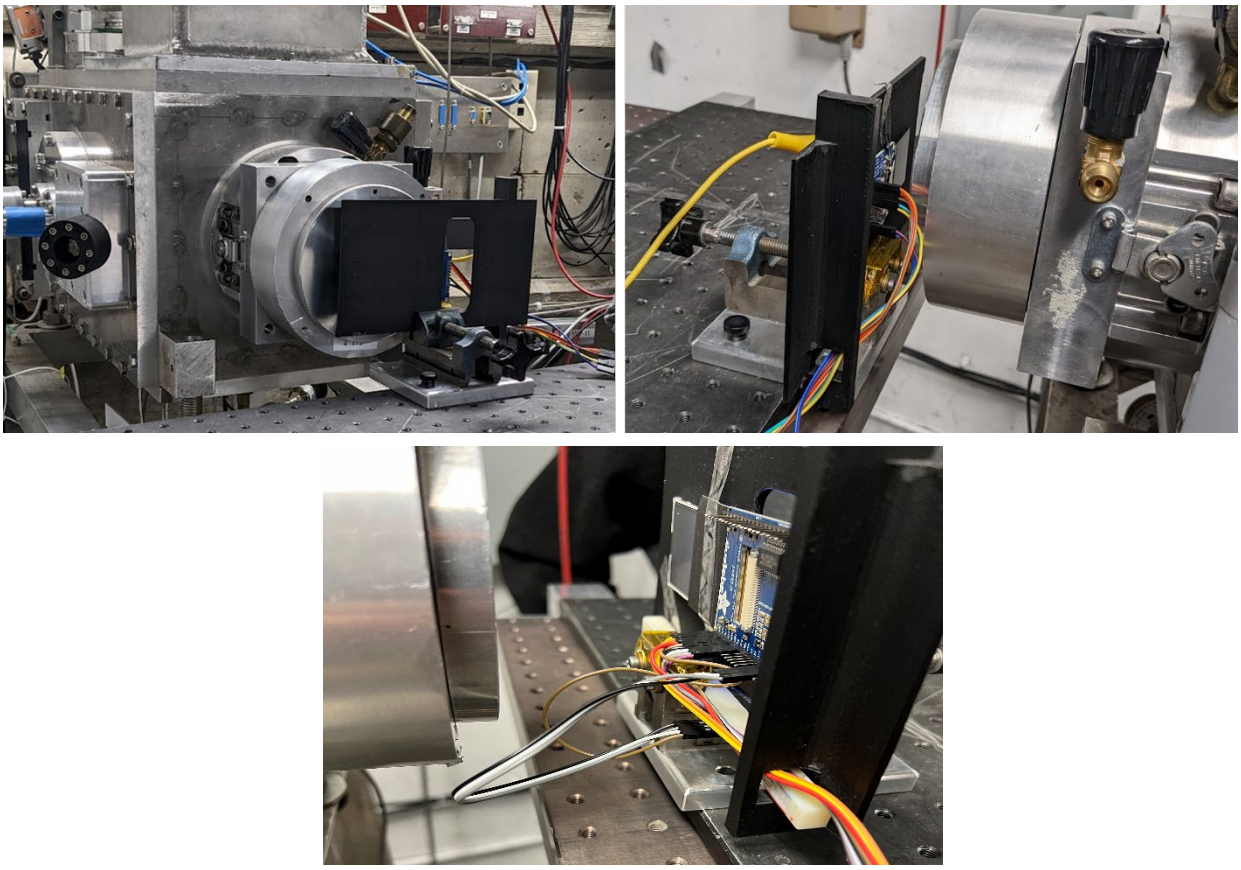

Figure 8: Test boards mounted for irradiation in the beam line.

Table 2: Arduino/Display Connections

LCD - SPI Connection		
Display Board Pin	**Connections**	**Functionality**
Vin	Arduino 5 Volt Output Port	Power
GND	Arduino Ground Port	Ground
CLK	Arduino Digital Pin 13	SPI Control
MISO	Arduino Digital Pin 12	SPI Control
MOSI	Arduino Digital Pin 11	SPI Control
CS	Arduino Digital Pin 10	Chip Select
D/C	Arduino Digital Pin 9	Data/Command Pin
RST	Arduino Digital Pin 8	TFT Reset
IM2	3Vo (Display Board Pin)	Enable SPI Configuration

OLED - SPI Connection		
Display Board Pin	**Connections**	**Functionality**
Vin	Arduino 5 Volt Output Port	Power
GND	Arduino Ground Port	Ground
CSLK	Arduino Digital Pin 2	SPI Control
MOSI	Arduino Digital Pin 3	SPI Control
DC	Arduino Digital Pin 4	Direct/Command Pin
OLEDCS	Arduino Digital Pin 5	Chip Select
RST	Arduino Digital Pin 6	Reset Pin

Electronic Paper - SPI Connection		
Display Board Pin	**Connections**	**Functionality**
Vin	Arduino 5 Volt Output Port	Power
GND	Arduino Ground Port	Ground
SCK	Arduino Digital Pin 13	SPI Control
MISO	Arduino Digital Pin 12	SPI Control
MOSI	Arduino Digital Pin 11	SPI Control
DC	Arduino Digital Pin 10	Data/Command Pin
ECS	Arduino Digital Pin 9	Chip Select Pin
RST	Arduino Digital Pin 8	Reset Pin
BUSY	Arduino Digital Pin 7	e-Ink Busy Pin
SRCS	Arduino Digital Pin 6	SRAM Select Pin

3. TEST DESCRIPTION

3.1. Optical Characterization

Notionally, electronic displays are intended to transmit to humans via the emission of photons that are in-turn transduced via photoreceptors in the eyes. One of the most fundamental optical characterizations for evaluating a light source is the optical spectrum of a light source, deconstructing a light source into spectral components across a defined wavelength domain (human vision is typically defined from 370 – 730 nm). Given that performance criteria for electron displays are evaluated from a human-user perspective, it is instructive to form the connection between traditional characterization metrics of microelectronics and optoelectronic devices and the metrics that are outlined in this report. The primary consideration would be the conversion of radiant energy output from an electronic display to the effective luminous energy transmitted to the eye for visual perception. This distinction is made as the photoreceptors in the eye are not uniformly sensitive to light and therefore not all energy output from a display is utilized in visual perception.

The "brightness" of a light source is characterized by luminous flux of the white light source (units of candelas or lumens). A luminosity function represents the spectral sensitivity of the average human eye as it relates to visual perception and is used as spectral "weight" to covert radial spectral flux (energy on a surface) to the something more akin to visual energy. The luminosity function that was used in the test report, in addition to a blue, green, and red screen from an electronic display, is provided in Fig. 9. The analysis within this report utilizes the photopic luminosity function to collapse optical spectra of an emissive electronic display into luminous quantities, but it should be noted that there are alternative luminosity functions that could be useful for more tailored applications. Meoscopic (twilight) and scotopic (low light)

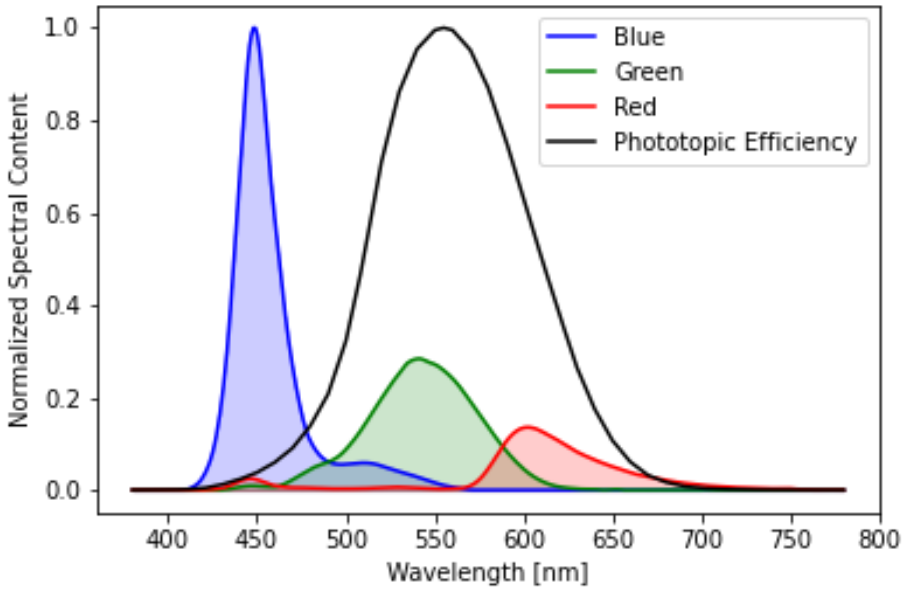

Figure 9: Spectra of a red, green, and blue pixel overlayed with the photopic efficiency function used to compute luminosity intensity of a light source. Note the significant spectral overlap of the photopic efficiency function with the green pixel.

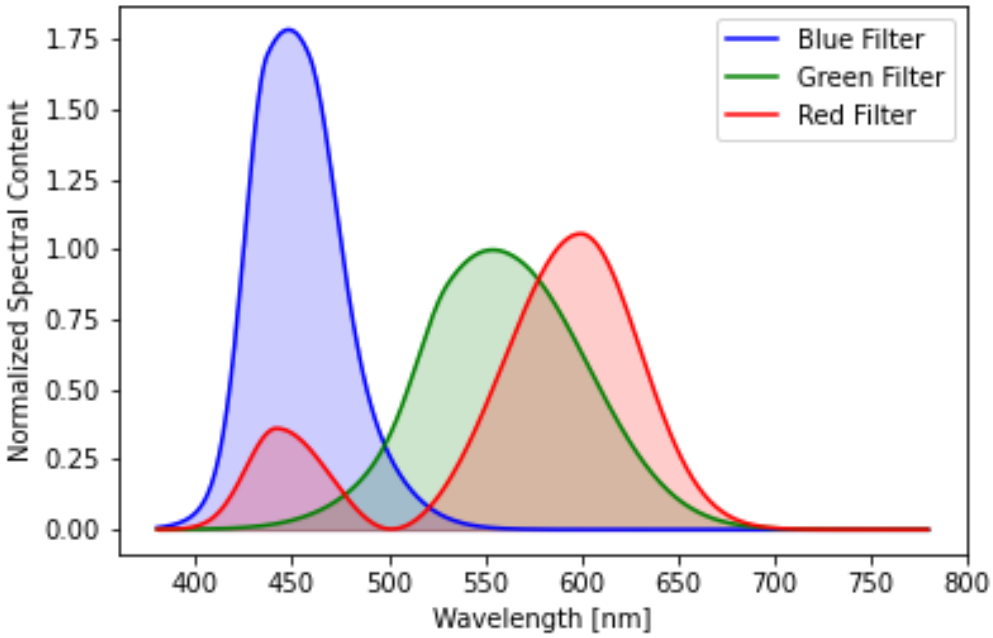

Figure 10: Spectral content of the color filters used to decompose an optical spectrum into tristimulus values used to define quantitative color theory.

luminosity functions can be used to define light constrained environments while protanopic and deuteranopia luminosity functions can account for atypical eye sensitivity to colors (e.g. color blindness). To first order these alternative luminosity functions are simply shifting the spectral center of the photopic luminosity function.

In addition to "brightness", wavelength-dependent sensitives of photoreceptors give rise to the visual perception of color. Viewed through the prism of color theory (pun intended), the "color" of a given optical spectra is parameterized by the three spectral sensitivities referred to as tristimulus values (provided in Fig. 10). These tristimulus values can then be used to compute two chromaticity values that can be mapped to a color space diagram to represent the color of a spectrum. It should be noted that the chromaticity analysis in this test report utilizes the process outlined by the International Commission on Illumination (CIE) in 1931, as the intent is to understand radiation-induced shifts in chromaticity, but color theory is an active community that has and will produce alternative color analysis tools that could be applied to these type of test results.

3.2. Test Setup

Individual display boards were attached to a mounting protoboard for irradiation. Each test board was connected via control and power wires to an Arduino microcontroller away from the proton beam where power supplies are typically placed. Displays were driven with monotonic black screens, monotonic white screens, or powered off (all pins grounded).

Following each irradiation step, the display boards and associated Arduinos were powered off to temporarily to relocate the irradiated board to a black box setup for optical characterization.

During characterization, the Arduino and the display board were powered with distinct power supply channels sourcing 5.2V. A variety of test images (all white, green, red, and blue) are uploaded to the microcontroller to drive the display for optical characterization. For each image, an optical spectrum was captured via the handheld spectrometer and stored for post processing. Care was taken to ensure consistent placement of the handheld spectrometer across measurements and dose steps.

As the display board was powered with a LabView controlled power source during characterization, current draw measurements of the entire display board were taken at each dose step. A test pattern of a solid color screen changing every five seconds (black, white, red, green, blue) was used during current draw measurements. It should be noted that these current draw measurements must include the display drive IC in addition to the display screen itself. In addition to the onboard power regulation protections of the Arduino and display boards, power supplies were set to a current compliance of 200 mA.

Table 3: List of Equipment

Equipment Name	Functionality
Arduino Microcontroller	Drive display boards
Sekonic c7000 Spectrometer	Spectrometer for optical characterization
Keithley 2230 Power Supply	Power display boards and Arduinos, measure current draw from the board.
Dell Lab Computer	Control power supply for measurements, upload microcontroller codes for testing
Assorted Cables	BNCs, USBs, copper wire, etc.

3.3.Irradiation Conditions

Testing was performed with 64 MeV protons at Crocker Nuclear Lab at the University of California – Davis. The test chamber during irradiation was room temperature (22.2 C˚) with a humidity of 37%. As protons must pass through glass and plastic overburden to reach the light emission and TFT layers, SRIM calculations [9] were performed to confirm that proton energies were not significantly impacted by the overlayers. Pre-irradiation measurements were taken for each display to provide a baseline to evaluate for radiation-induced degradation after each radiation dose. Irradiation steps were selected in accordance with mission dose requirements and to characterize device sensitivity for future applications (provided in Table 4). Measurements were taken at least fifteen minutes after irradiation to allow for short term annealing of defects.

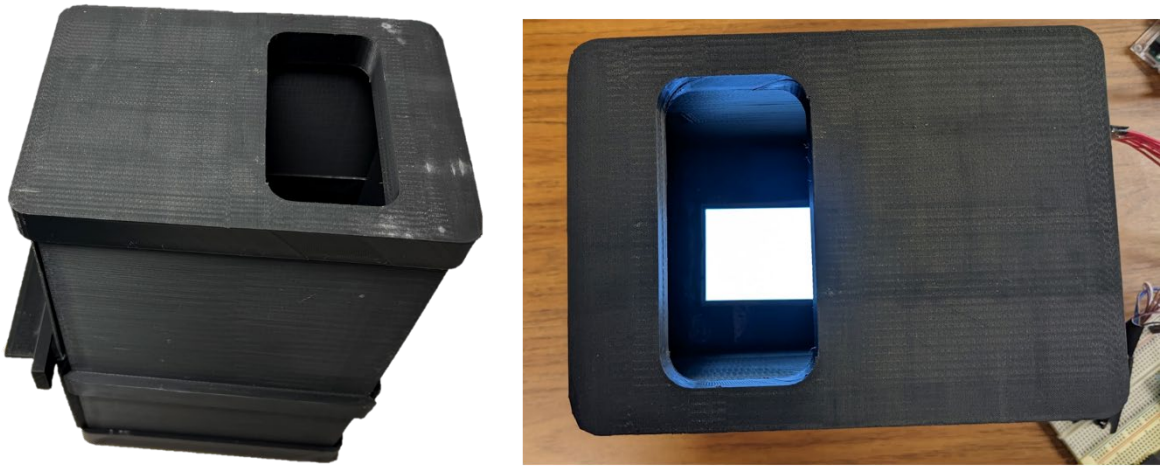

Figure 11: A picture of the light box and display board measurement setup. Note that the light box fits over the display board.

Table 4: Irradiation Conditions

Label	Technology	Irradiation Condition	Total Ionizing Dose [krad (Si)]	64 MeV Proton Fluence [10^{10} p^+/cm^2]
LCD1	LCD	Black	0, 50, 100, 150	0, 86, 172, 257
LCD2	LCD	White	0, 50, 100, 175	0, 86, 172, 300
LCD3	LCD	Black	0, 10, 20	0, 17, 34
LCD4	LCD	White	0, 10, 20, 30	0, 17, 34, 51
LCD5	LCD	White	0, 10, 30, 50, 70, 100	0, 17, 51, 86, 120, 172
OLED1	OLED	Black	0, 10, 20, 30, 40, 50, 100, 125	0, 17, 34, 51, 69, 86, 172, 215
OLED2	OLED	Pins Grounded	0, 10, 20, 30, 40, 75	0, 17, 34, 51, 69, 129
OLED3	OLED	Black	0, 50, 100, 150, 200	0, 86, 172, 257, 343
OLED4	OLED	White	0, 50, 150	0, 86, 257
BLED	Blue LED	Pins Grounded	0, 10, 30, 50, 100, 150, 250, 300	0, 17, 51, 86, 172, 257, 429, 515
WLED1-3	White LED	Pins Grounded	0, 20, 40, 60, 80, 100	0, 34, 69, 103, 137, 172
MINK	Monochrome eInk	Pins Grounded	0, 100, 200	0, 172, 343
TINK	Tricolor eInk	Pins Grounded	0, 100, 200	0, 172, 343

4. RESULTS

Overall, radiation-induced degradation was observed for each emissive pixel technology examined in this report. However, the doses used in these tests are significant and would likely equate to several years on the lunar surface applications while quantitative degradation (in the range of 10 – 20%) would likely be tolerable within a typical mission concept-of-operation.

Given that an objective of these tests was to preliminary examine the radiation-induced degradation in various pixel technologies, it is useful to consider what is being irradiated in each display type to better understand potential degradation mechanisms for each test display and generalize the results.

- Edge Coupled TFT-LCD: thin film transistor back plane, liquid crystals, filters, plastic overlayers
- Passive Matrix OLED: OLED, glass overlayers, backside conductive network
- Monochromatic LED Matrices: LEDs, coating, plastic overlayers, backside conductive network

The fact that radiation-induced degradation was observed in all three display types without a common design feature implies that display screens have multiple potential degradation mechanisms that should be considered for a candidate display.

4.1. Active Matrix TFT-LCD with Side Coupled LED Backlight

Given the widespread use of LCDs and TFT backplanes for high performance displays, it is pragmatic to start with the TFT-LCD display boards examined in this report. Starting with the luminosity of a white screen, Fig. 12 demonstrates radiation-induced luminosity degradation as function of dose; it should be noted that there is not an apparent dependence on the screen used during irradiation. While a white screen results in the largest luminosity of the screen for nominal operation, color displays provide a whole gamut of color to a system, so it is useful to characterize radiation-induced degradation of the constitutive colors (red, green, blue). Luminous intensity of monotone red, green, and blue screens were measured at each dose and shows distinct sensitivities for each color (Fig. 13). This behavior can be confirmed via examination of the raw optical spectra captured from the display which shows that degradation is not uniform across the wavelength range (Fig. 14). A direct consequence of this non-uniformity is a shift in perceived color as the color mixing ratio of the display becomes perturbed as a function of dose. This shift in color is portrayed on chromaticity diagram (Fig. 15).

It should be noted that LCD3 and LCD4 functionally are reported to a significantly lower dose than other displays of the same type due to early functional failure of the display. It was suspected the root cause of the failure was accidental exposure of the display driver IC during a dose step. An intentional exposure of the display driver IC on another display showed similar functional failure around 20 krad (Si) to provide anecdotal support for the early failure.

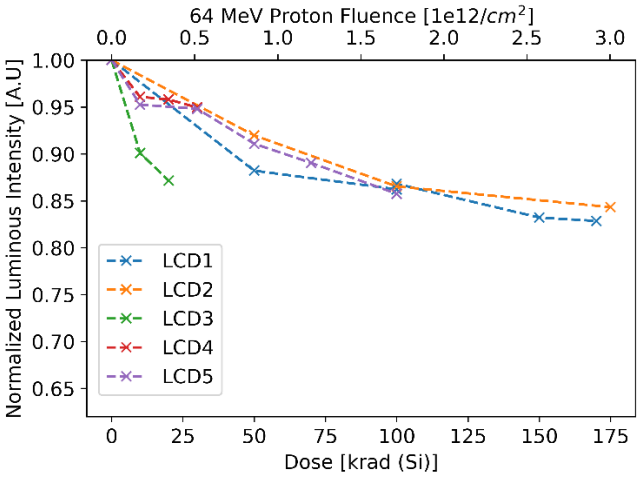

Figure 12: Luminosity intensity of a white screen normalized to pre-rad values for the LCDs examined in this measurement campaign. Note that LCD4 and LCD5 were rendered inoperable likely due to inadvertent irradiation of the driver IC.

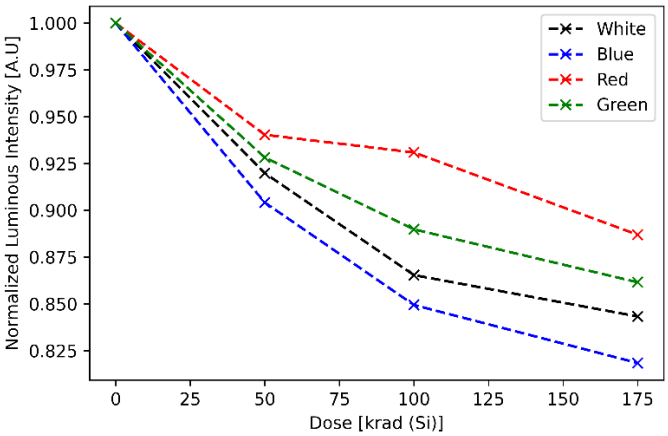

Figure 13: Luminosity intensity normalized to pre-rad values for red, green, blue, and white screens for LCD2. Note pixel colors degrade at a distinct rate. This behavior was consistent across all LCDs in this measurement campaign.

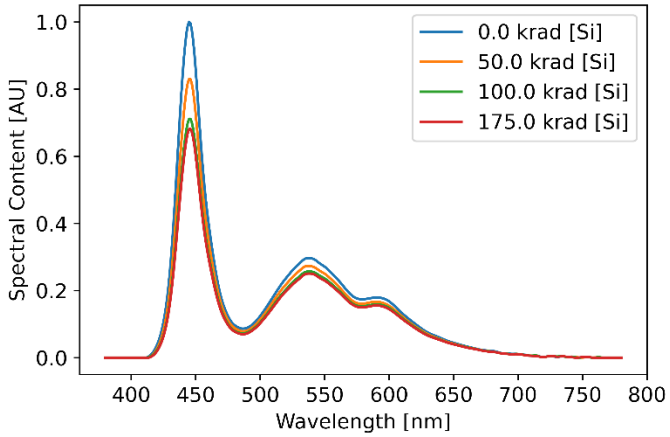

Figure 14: Spectra of a white screen as a function of dose for LCD2. Note that the degradation is wavelength-dependent, confirming the results shown in Fig. 13.

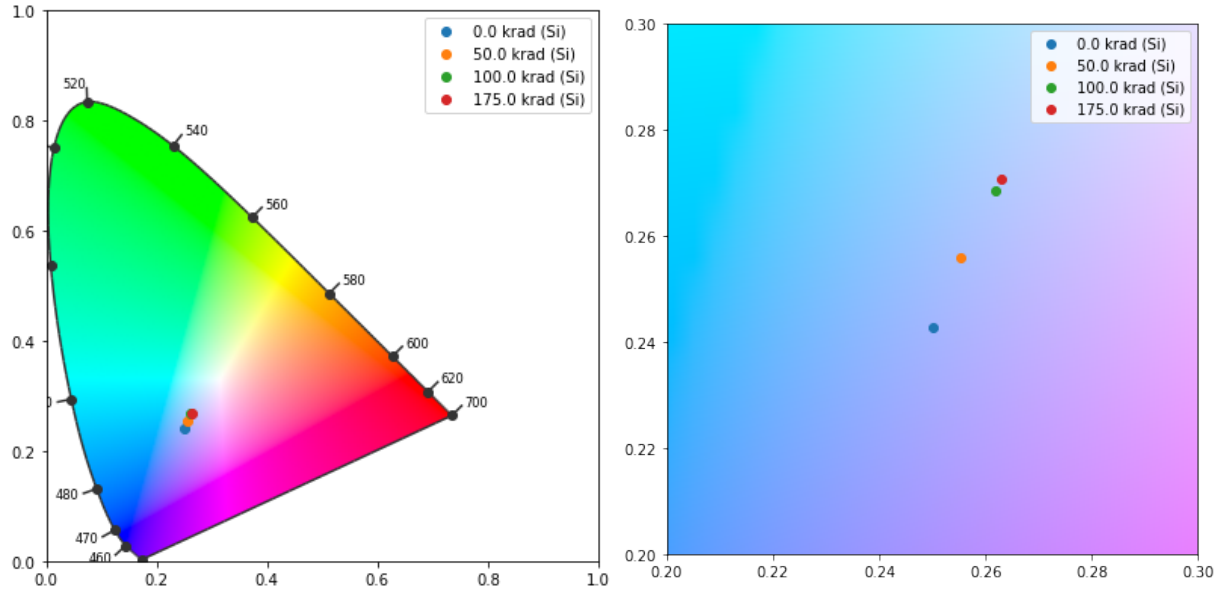

Figure 15: CIE 1931 color space diagram to show radiation-induced color shift in white screen for LCD2. Note the direction of the shift is towards a yellowing.

4.2. Passive Matrix OLED

For the optical characterization of the OLEDs, it can be seen that there is a decrease in the luminosity as a function of dose/particle fluence for the displays independent of the screen during irradiation (Fig. 16). Reviewing the luminosity degradation of the constituent pixel colors, there is a color-dependent luminosity degradation consistent with the behavior observed in the LCDs. This color-dependent luminosity will in-turn impact color mixing which can be shown by reviewing the color space diagram for the displays. As this behavior was consistent across the displays, Fig. 17 displays the optical spectra for OLED3 as a demonstration.

Current draw for the entire display board was conducted at each dose step with some representative current traces from OLEDX and OLED is provided in Fig. 18. Current traces are taken for a repeating test pattern (black-red-green-blue-white) with each current plateau corresponding to a screen color (black is lowest current draw). There is negligible shift in current draw as a function of dose; this behavior is seen across all the OLED displays examined in this report. It should be noted that each current trace was manually shifted on the x-axis of the plots for comparison so there is no significance to slight misalignment of the traces.

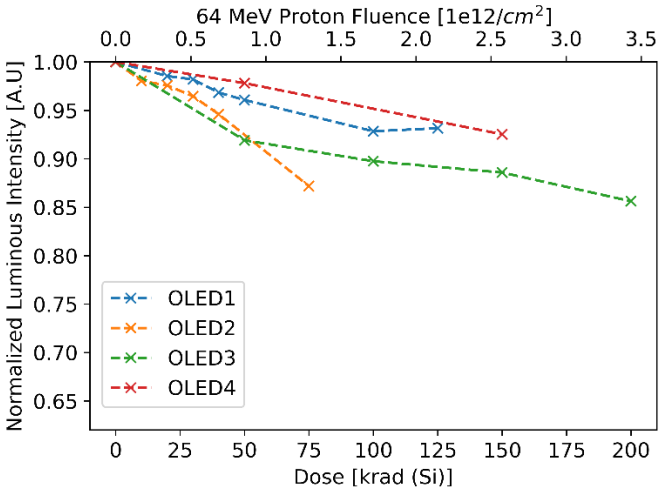

Figure 16: Luminosity intensity of a white screen normalized to pre-rad values for the OLEDs examined in this measurement campaign.

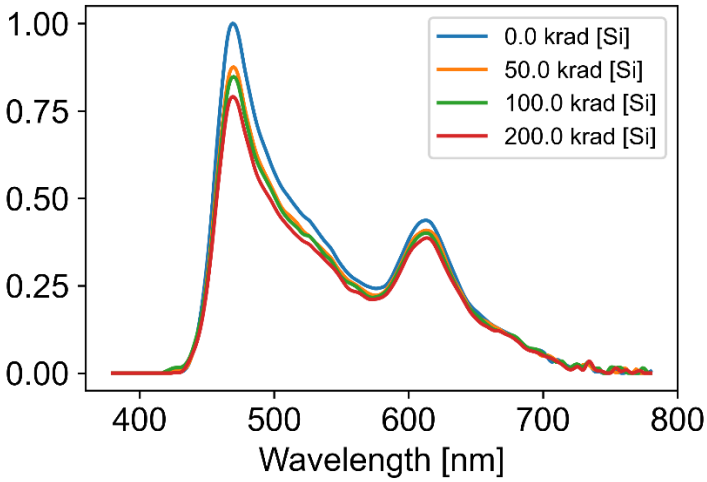

Figure 17: Spectra of a white screen as a function of dose for OLED3. Note that the degradation is wavelength-dependent.

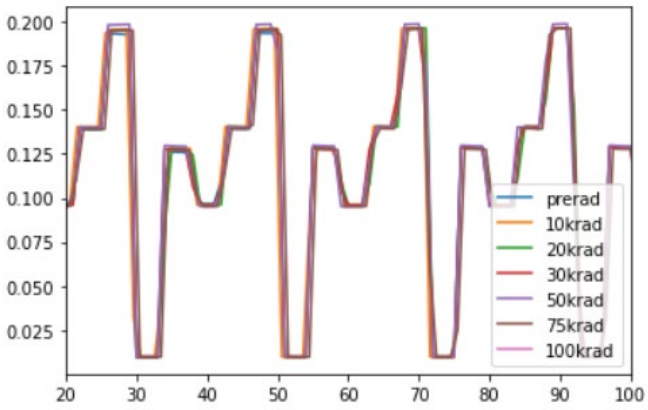

Figure 18: Current traces of OLED during a test pattern of black-red-blue-green-white. Note that the traces were shifted along x-axis (time) so discrepancies are insignificant.

4.3. Monochromatic LED Dot Matrices

As the dot matrix LEDs are monochromatic, the optical and electrical characterization are performed with single test images: all LEDs biased on to 2.5V. For the optical characterization of the LEDs, it can be seen that there is a decrease in the luminosity as a function of dose/particle fluence for both the blue and white LEDs (Fig. 19). It is informative to review the optical spectra as a function of dose which shows a rather uniform attenuation across the optical spectrum (Fig. 20 – 21). This uniform degradation should maintain consistent color mixing and that inference is confirmed via review of the color space diagram for the LEDs (Fig. 22). Since the white light produced of the LED is produced by a coating as opposed to the production of white light from the combination of sub-pixel colors, it is reasonable to infer that the process of color mixing results in the shift of color as opposed to a wavelength-dependent degradation mechanism such as color centers in plastic overlayers.

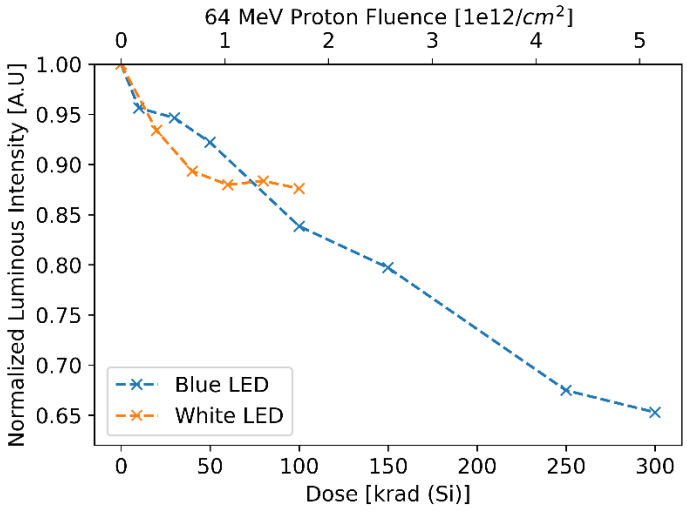

Figure 19: Luminosity intensity normalized to pre-rad values for the LED matrices examined in this measurement campaign. Note that white LED is the average of three DUTs.

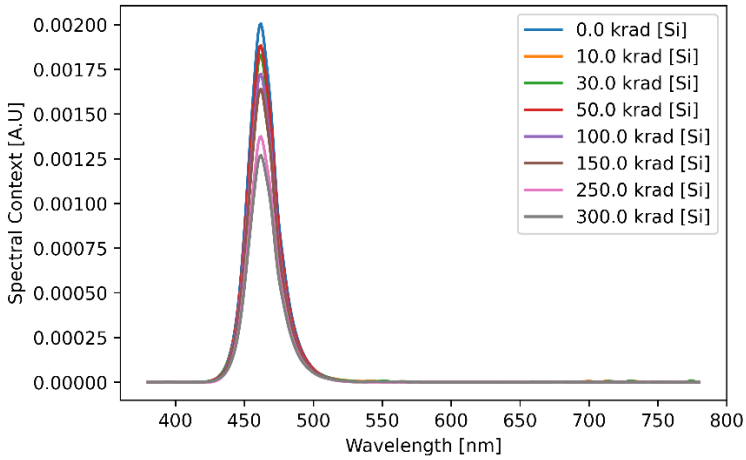

Figure 20: Spectra as function of dose for the blue LED. Note that the degradation is largely uniform across the wavelength range of interest.

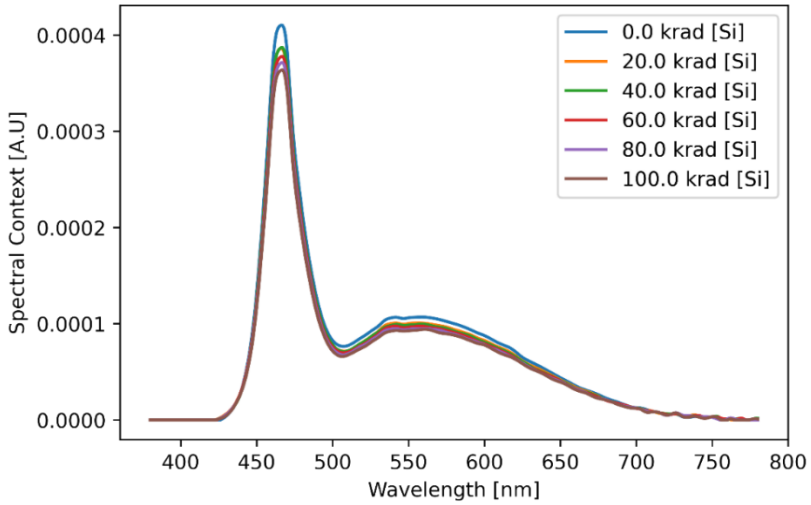

Figure 21: Spectra as function of dose for the white LED. Note that the degradation is largely uniform across the wavelength range of interest.

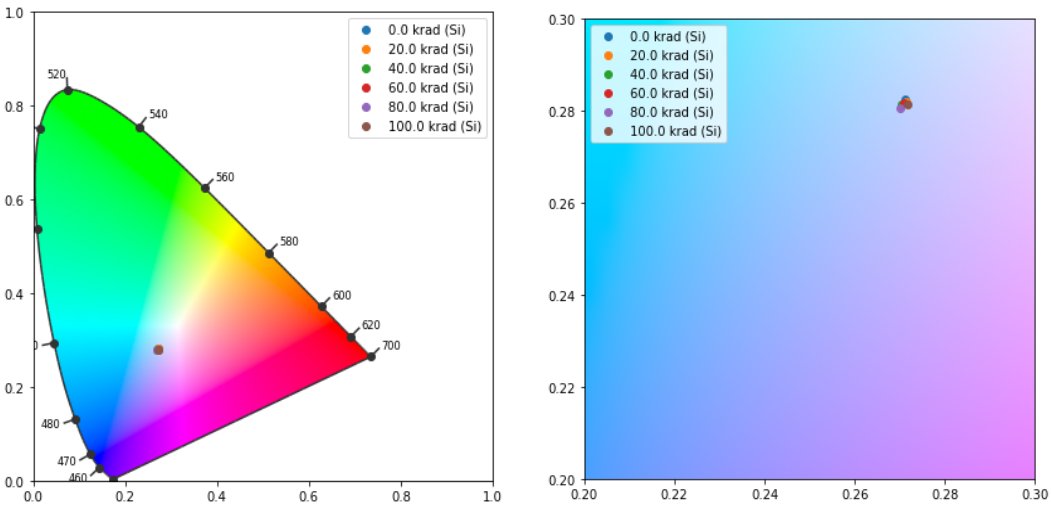

Figure 22: CIE 1931 color space diagram to show color in the white LEDs as a function of dose. Note the lack of color shift observed in the white LEDs.

4.4. Electronic Paper/Ink

As the electronic paper displays are reflective (contain no emissive instruments), it was not possible to utilize the handheld spectrometer to directly monitor optical spectra of the display. Rather than actively driving the display with an Arduino, a persistent test image was uploaded to the display board and then irradiated with all pins grounded. The electronic displays were irradiated with 50 krad (Si) dose steps up to a total dose of 200 krad (Si) without presenting any visual degradation of the test image (e.g. no erroneous pixels). It should be noted that quantitative measurements analogous to the spectrometer measurements for the emissive displays would likely require additional optical techniques such as spectrographic reflectometry measurements.

5. SUMMARY

A 64 MeV proton irradiation campaign was carried out on COTS display pixel technologies (LCDs, OLEDs, LEDS, and eInks) to provide a preliminary examination of sensitives in anticipation of future crewed applications. Display boards were modified to prevent irradiation of support electronics and confine any radiation-induced degradation to the pixel component of the display board. Pixel technologies were irradiated to an excess of 100 krad (Si)/1.72x10^{12} p^{+}/cm^{2} (64 MeV) with the corresponding optical response characterized utilizing a handheld spectrometer (Table 5). While there was measurable degradation at these doses (in the range of 10 – 20%), typical applications would results in significantly lower doses and therefore less degradation.

Table 5: Comparison of Pixel Technologies at 100 krad [Si].

Device Label	100 krad(Si) Test Dose - White Screen		
	64 MeV Proton Fluence	Total Ionizing Dose	Normalized Luminous Intensity Degradation
LCD-1	1.72E+12	100 krad(Si)	86.50%
LCD-2			86.70%
LCD-3			Driver IC inoperable after accidental irradiation
LCD-4			
LCD-5			90.00%
OLED-1	1.72E+12	100 krad(Si)	89.80%
OLED-2			92.50%
OLED-3			93.20%
OLED-4			83.60%
WLED-1	1.72E+12	100 krad(Si)	87.70%
WLED-2			82.50%
WLED-3			91.90%
BLED-1	1.72E+12	100 krad(Si)	83.80%
MEINK-1	1.72E+12	100 krad(Si)	No visual degradation observed
TEINK-1	1.72E+12	100 krad(Si)	No visual degradation observed

6. REFERENCES

[1] Adafruit, “OLED Breakout Board - 16-bit Color 1.5" w/microSD holder,” Accessed: May 2022. [Online].Available: https://www.adafruit.com/product/1431

[2] Adafruit, “Adafruit 2.4" TFT LCD with Touchscreen Breakout w/MicroSD Socket - ILI9341,” Accessed: May 2022. [Online].Available: https://www.adafruit.com/product/2478

[3] Adafruit, “3.5" TFT 320x480 + Touchscreen Breakout Board w/MicroSD Socket - HXD8357D,” Accessed: Sept. 2022. [Online].Available: https://www.adafruit.com/product/2050

[4] Adafruit, “Adafruit 1.54" Monochrome eInk / ePaper Display with SRAM - 200x200 with SSD1681,” Accessed: Sept. 2022. [Online].Available: https://www.adafruit.com/product/4196

[5] Adafruit, “Adafruit 1.54" Tri-Color eInk / ePaper 200x200 Display with SRAM - SSD1681 Driver,” Accessed: Sept. 2022. [Online].Available: https://www.adafruit.com/product/4868

[6] Adafruit, “Small 1.2" 8x8 Ultra Bright Blue LED Matrix - KWM-30881CBB,” Accessed: Sept. 2022. [Online].Available: https://www.adafruit.com/product/1047

[7] Adafruit, “Miniature Ultra-Bright 8x8 White LED Matrix,” Accessed: Sept. 2022. [Online].Available: https://www.adafruit.com/product/1079

[8] M. Shaw, M. Fairchild, "Evaluating the 1931 CIE color‐matching functions", *Color: Research and Application.,* vol. 27, no. 5, pp. 316–329, Oct. 2002.

[9] J. F. Ziegler, "SRIM - The Stopping and Range of Ions in Matter," Accessed: May 2022. [Online]. Available: http://www.srim.org/

7. APPENDICES

7.1 Active Matrix TFT-LCD with Side Coupled LED Backlight - Spectra

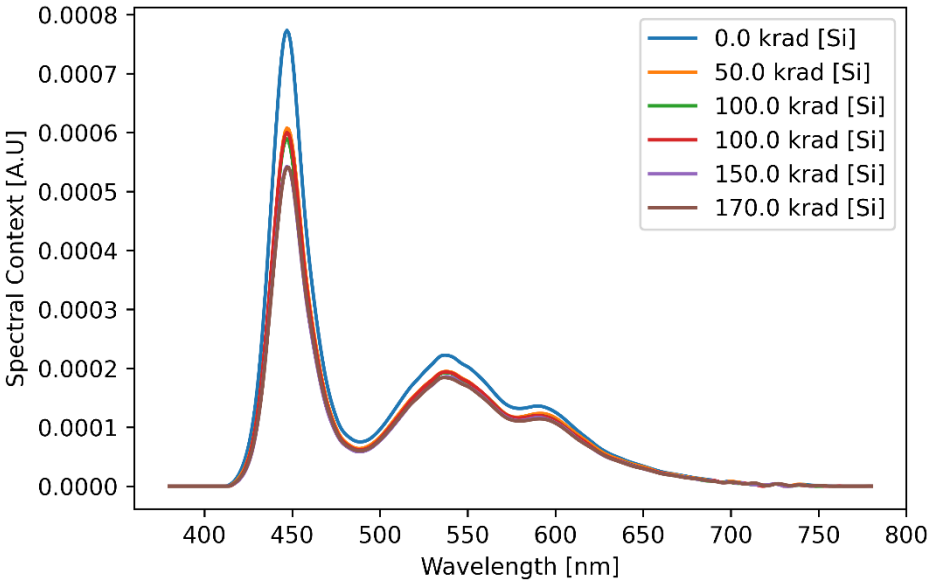

Figure 23: Spectra of a white screen as a function of dose for LCD1.

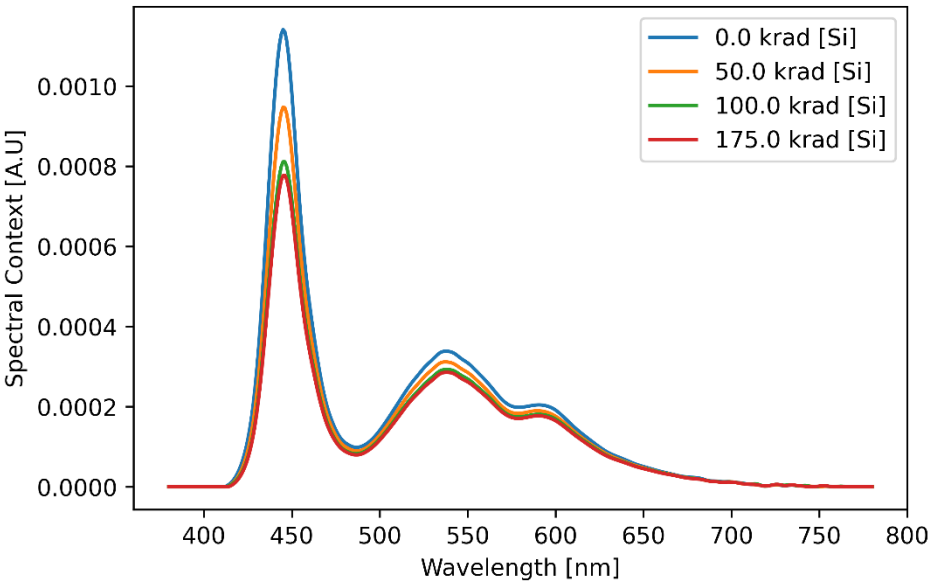

Figure 24: Spectra of a white screen as a function of dose for LCD2.

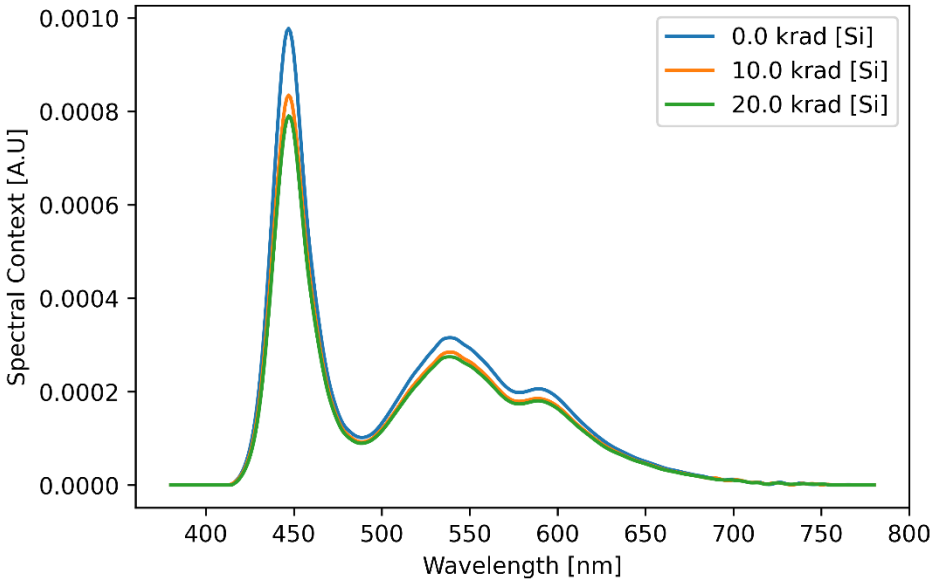

Figure 25: Spectra of a white screen as a function of dose for LC3

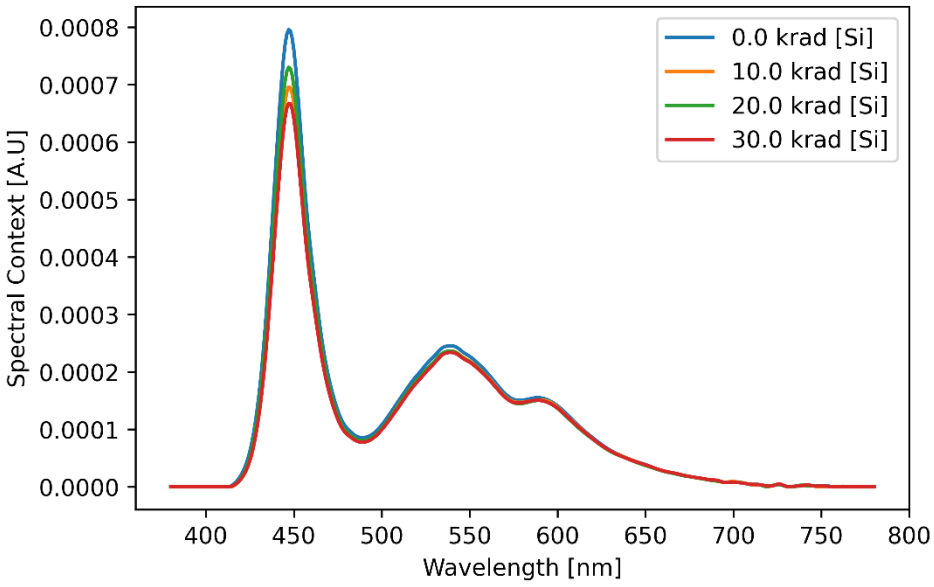

Figure 26: Spectra of a white screen as a function of dose for LCD4.

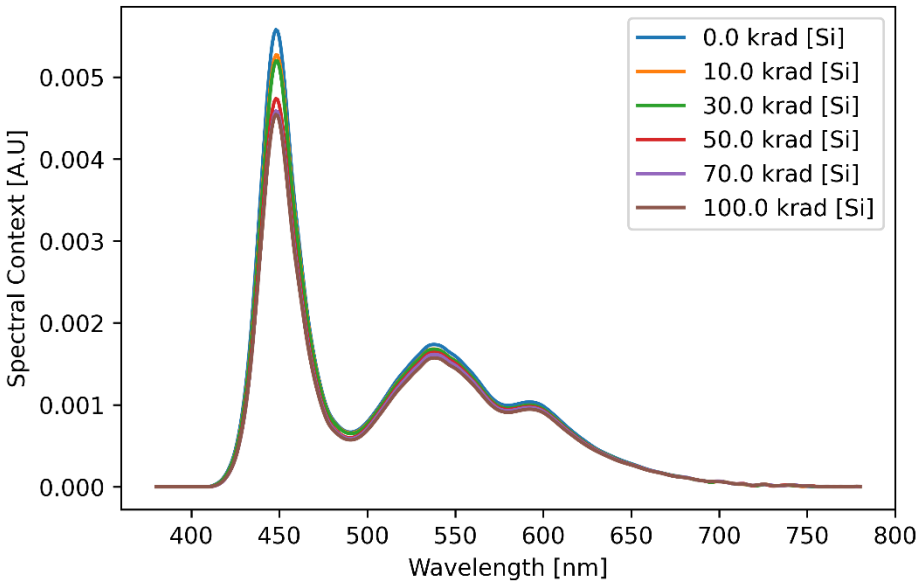

Figure 27: Spectra of a white screen as a function of dose for LCD5.

7.2 Passive Matrix OLED – Spectra

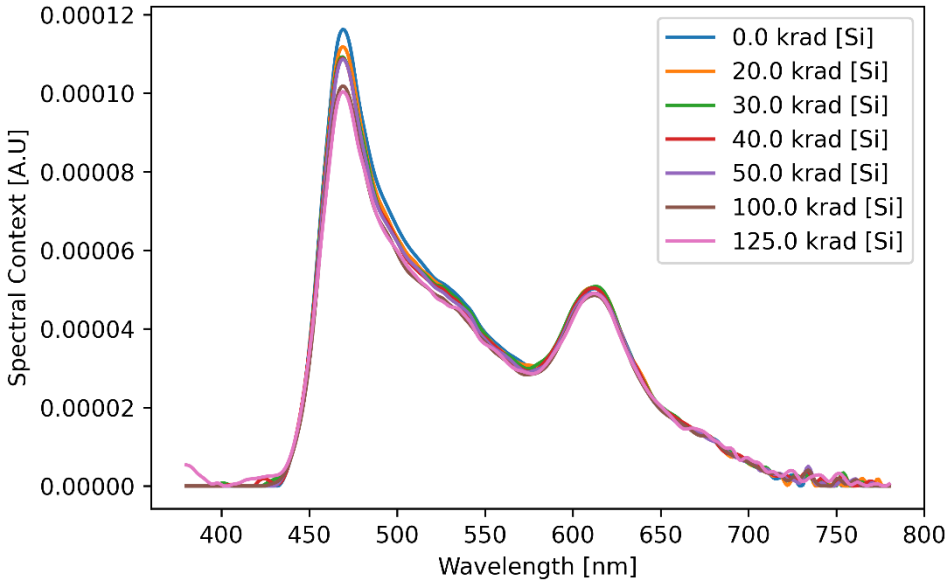

Figure 28: Spectra of a white screen as a function of dose for OLED1.

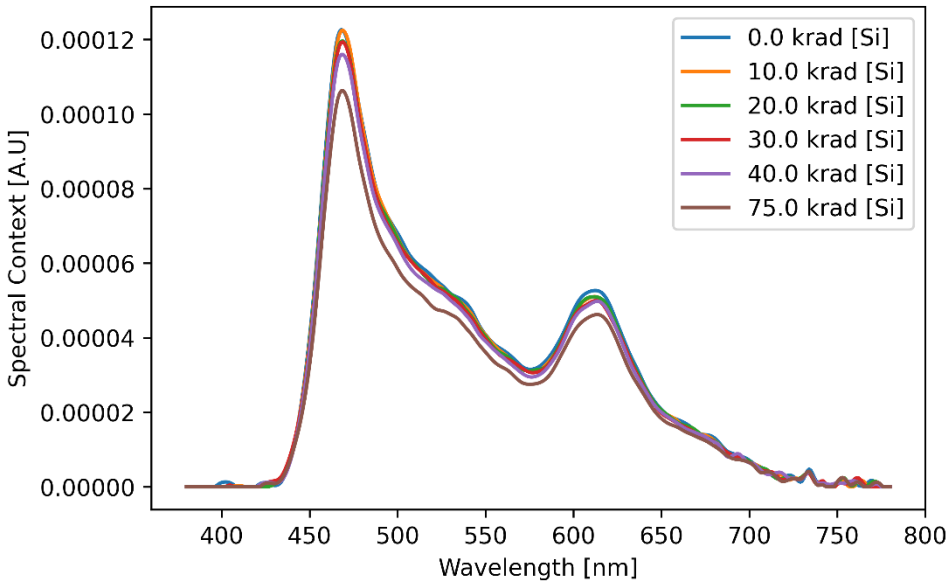

Figure 29: Spectra of a white screen as a function of dose for OLED2.

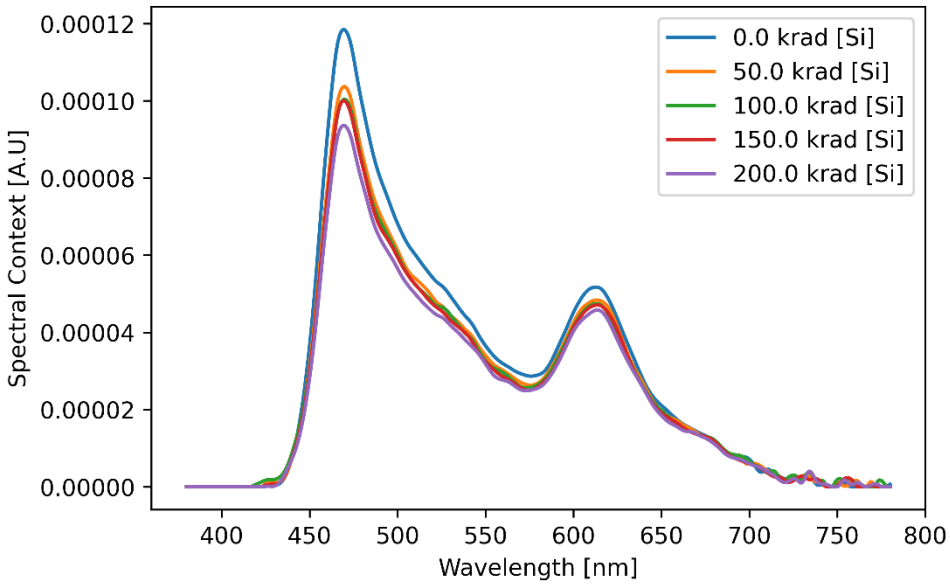

Figure 30: Spectra of a white screen as a function of dose for OLED3.

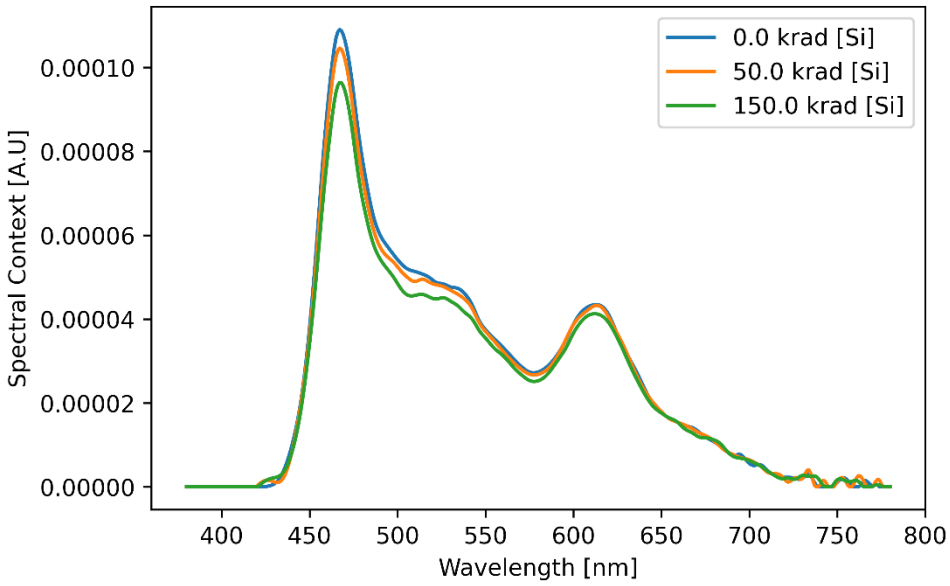

Figure 31: Spectra of a white screen as a function of dose for OLED4.